D_i^* and N_i alone,

$$f_v = 1 - (2/M_0)[\sum_i N_i D_i^* \psi_i (D_i^* - \bar{D}^*)/ \bar{D}^* \sum_i N_i D_i^* \psi_i], \quad (60)$$

where

$$\psi_i = [M_0 \bar{D}^* - 2(D_i^* - \bar{D}^*)]^{-1}. \quad (61)$$

This becomes for a random binary alloy,

$$f_v = 1 - \frac{2}{M_0} \frac{(M_0+2) N_A N_B (D_A^* - D_B^*)^2}{(M_0+2)(\bar{D}^*)^2 - 2D_A^* D_B^*}. \quad (62)$$

Values of f_v for a binary alloy calculated from Eq. (62) are shown in Fig. 6. These values differ slightly from approximate values shown previously.[4,5] In Ref. 5, an approximation was introduced by the assumption that H equaled H_0. This approximation is important when f_v is small. In Ref. 4, an error was made in the numerical computation of the f_v values.

By definition, the atom correlation factor f_A for the faster-diffusing species in a random binary alloy goes to zero at the boundary of the forbidden region. This is illustrated in Fig. 1. Also, Fig. 6 shows that the vacancy correlation factor in a random binary alloy goes to zero at the boundary of the forbidden region. This general result can be demonstrated from Eqs. (55) and (62).

At the boundary of the forbidden region, Eq. (55) yields

$$D_B^* = D_A^*(1 - f_0 N_B^{-1}). \quad (63)$$

Substituting this into Eq. (62) with f_0 equal to $M_0/(M_0+2)$, as shown by Eq. (14), and $\bar{D}^*$ equal to $N_A D_A^* + N_B D_B^*$ yields the result $f_v = 0$ for all values of N_A.

It would be interesting to compare experimental values of f_v with Eq. (60) or (62). In principle, the equation

$$D_v = \tfrac{1}{6} \lambda^2 W f_v z \quad (64)$$

would allow f_v to be determined experimentally in an alloy where D_v and W could be measured. No such measurements are available, however.

[1] J. R. Manning, Phys. Rev. 116, 819 (1959).
[2] J. R. Manning, *Diffusion Kinetics for Atoms in Crystals* (Van Nostrand, Princeton, N. J., 1968).
[3] J. R. Manning, Z. Naturforsch. 26, 69 (1971).
[4] J. R. Manning, Acta Met. 15, 817 (1967).
[5] J. R. Manning, in *Lattice Defects and Their Interactions*, edited by R. R. Hasiguti (Gordon and Breach, New York, 1967), p. 267.
[6] A. D. LeClaire, Phil. Mag. 3, 921 (1958).
[7] J. R. Manning, Met. Trans. 1, 499 (1970).
[8] See for example, L. W. Barr and A. D. Le Claire, Proc. Brit. Ceram. Soc. 1, 109 (1964); L. W. Barr and J. N. Mundy, in *Diffusion in Body-Centered Cubic Metals*, edited by J. A. Wheeler, Jr. and F. A. Winslow (American Society for Metals, Metals Park, Ohio, 1965), p. 171.
[9] Th. Heumann and W. Reerink, Acta Met. 14, 201 (1966).
[10] W. A. Johnson, Trans. Am. Inst. Mining Met. Engr. 166, 114 (1946).
[11] K. Monma, H. Suto, and H. Oikawa, J. Japan Inst. Metals 28, 192 (1964).
[12] N. L. Peterson and S. J. Rothman, Phys. Rev. 154, 558 (1967).
[13] A. B. Kuper, D. Lazarus, J. R. Manning, and C. T. Tomizuka, Phys. Rev. 104, 1536 (1956).
[14] N. L. Peterson and S. J. Rothman, Phys. Rev. B 2, 1540 (1970).
[15] S. G. Fishman, D. Gupta, and D. S. Lieberman, Phys. Rev. B 2, 1451 (1970).

PHYSICAL REVIEW B VOLUME 4, NUMBER 4 15 AUGUST 1971

Multiband Model for the Electronic Heat Capacity of Chromium

J. F. Goff
Naval Ordnance Laboratory, White Oak, Silver Spring, Maryland 20910
(Received 15 December 1970)

The anomalous high-temperature values of the electronic heat capacity of Cr have been analyzed by a multiband model of the density of states with a nonstandard distribution of states about the Fermi level. This model was obtained from analysis of the anomalous high-temperature values of the conductivities without use of rigid-band arguments. The agreement of the model with the data not only explains their anomalous values but confirms that the anomalies in the conductivities are the result of band structure.

I. INTRODUCTION

It has been recently pointed out that the anomalous high-temperature Lorenz number of chromium ($L = k/\sigma T$, where k is the thermal conductivity, σ is the electrical conductivity, and T is the temperature) seems to depend upon the peculiar characteristics of the density of states of that metal.[1-3] A

model was derived from the analysis of these data that conforms to the known multiband characteristics of the electronic states of chromium[4,5]: It has a standard-band type-A surface that undergoes a BCS-type transformation below the Néel temperature ($T_N = 312$ K) and a nonstandard-band P surface that remains unchanged. The parameters of this model agree well with other experiments[6,7] and theory.[8]

However good that agreement may be since L is composed of transport coefficients, it and the model explaining it would be expected to be sensitive to scattering processes. In this particular case it was argued in some detail that the temperature dependence of the scattering process would cancel from the model. However, the energy dependence of the scattering would be left; and in spite of the agreement of the model with the known electronic structure of chromium there remained some uncertainty of its independence of the scattering process.

It was realized at the time[3] that if the predominant energy dependence of the model was truly representative of that of the density of states, then there could be anomalies in the high-temperature electronic specific heat that correlate with it because the specific heat is not dependent upon scattering. The purpose of this paper is to show that such a correlation does exist. The high-temperature electronic specific heat has a temperature dependence over a temperature range of nearly 1000 K that is predicted by the form of the P surface—a temperature dependence that is quite different from that of a simple minimum in the density of states. In this way it is shown that the anomalies in the high-temperature conductivities of chromium are a result of its peculiar band structure and not peculiar scattering.

There is an interesting secondary conclusion coming from this correlation of the anomalous Lorenz number and heat-capacity data, for in general it is not necessary for these quantities to correlate at all. The familiar Mott model[9] with its lightly populated s band and heavily populated d band presupposes that they do not. The correlation in the present case supports the contention that there are no dense d bands in Cr.[10,11]

It has been known for some time that the electronic heat capacity of chromium is abnormally large at high temperatures[12] and that this abnormal value is in some way associated with the Cr band structure.[13] Shimizu, Takahashi, and Katsuki[14] made such an analysis in terms of a single nonstandard band in which the density of states had been derived by a rigid-band analysis of the low-temperature electronic heat capacity of a series of Cr-V and Cr-Fe alloys. The results of their calculation reproduced some of the qualitative features of the data, but not all, and not their magnitude. The present calculation is consistent with that of Shimizu and coworkers in spirit but has the advantage that the distribution of states is obtained for Cr without the assumption of a rigid band.

Although the model will initially appear to consist of only two bands, it will be seen ultimately that it represents a more complicated structure. It differs from the usual band models in that all energies are referred to the Fermi level rather than a band edge. In fact the success of the model in the case of the conductivities indicates that there are no band edges near the Fermi level except, of course, in the case of the BCS-type gap that opens over the A surface. In order to take advantage of this fact, the electronic heat capacity will be reformulated in terms of this new reference energy. Since the model is completely symmetrical about the Fermi level, this formulation affords a great simplification in the analysis.

The data to be analyzed come from the American Institute of Physics Handbook[15] except in the neighborhood of T_N where the data of Beaumont, Chihara, and Morrison are used.[16] Unfortunately, one cannot be certain of the separation of the heat-capacity data into its various components below about 400 K. Therefore there has been no attempt to analyze these lower-temperature data in detail, although it is shown that they are qualitatively consistent with the model.

II. DATA

A. Corrections

The data[15,16] for the molar specific heat of Cr at constant pressure C_p are shown in Fig. 1 where they are plotted in units of J/mole deg. The data have been terminated at 1500 K because of the approaching melting point at somewhat higher temperatures.[17] These data do not interpolate simply through T_N, a problem that will be seen to be more complicated than the simple disappearance of a portion of the Fermi surface that has been so thoroughly studied by Heiniger and co-workers.[18,19] This interpolation problem is mitigated to some extent by correction of the data to the molar specific heat at constant volume C_v.

As is well known[20] the difference between these two heat capacities is

$$C_p - C_v = TV\beta^2/\kappa \ , \qquad (2.1)$$

where T is the temperature, β is the volume expansion, and κ is the volume compressibility. In the following V is taken to be the molar volume so that the C's become the molar specific heats.

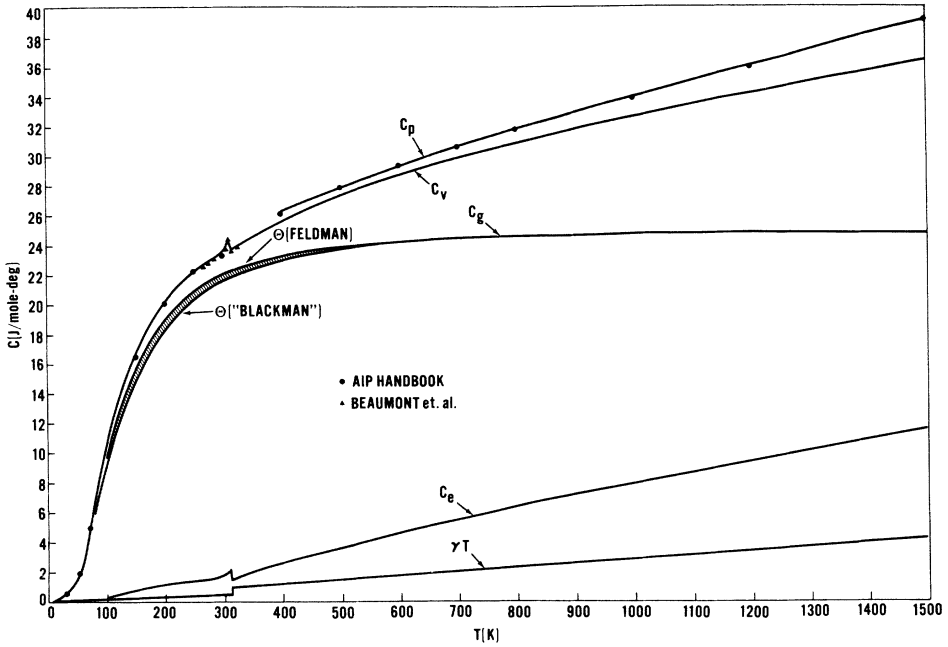

FIG. 1. Data for the heat capacity of Cr and their corrections. C_p are the data taken from the sources noted. C_v are this data corrected to constant volume. C_g is the lattice heat capacity calculated by two different Debye temperatures Θ. C_e is the electronic heat capacity obtained by substracting $C_v - C_g$. γT is C_e in its linear approximation obtained by using known values of γ at low temperatures.

The data for the right-hand side of this equation are not well known over the whole temperature range. It is a consequence of Grüneisen's law[20] that

$$A = V\beta^2/\kappa C_p^2 \qquad (2.2)$$

is approximately constant for solids. In this way Eq. (2.1) is transformed into the Nernst-Lindemann equation

$$C_p - C_v = AC_p^2 T \ , \qquad (2.3)$$

which has been used to transform the data to C_v in Fig. 1.

Since the antiferromagnetic transformation at T_N affects the properties of Cr markedly, the constant A is shown in Table I evaluated at 200 and 400 K. It has been assumed that the molar volume, which was evaluated from the density given in Sully[17] is constant over this temperature range. The values of β were found by assuming that it is three times the measured linear expansion.[21] Bridgman's data[22] were extrapolated to zero pressure to give the values of κ. The difference in the value of A above and below T_N shown in Table I is somewhat pedantic because the transformation becomes unimportant at the lower temperatures.

B. Lattice Component

There are possibly three components of C_v: the lattice contribution C_g, the electronic contribution C_e, and the spin contribution C_s. Feldman[23] has argued that C_s is negligible. Therefore C_e can be found by subtracting calculated values of C_g from C_v.

C_g shown in Fig. 1 was calculated from the usual Debye formula

$$C_g = 9R_g(T/\Theta)^3 \int_0^{\Theta/T} [x^4 e^x/(e^x - 1)^2]\,dx \ , \qquad (2.4)$$

where R_g is the gas constant and Θ is the Debye temperature. Θ must be a function of T in order to make this equation conform to reality.

The low-temperature value of Θ is uncertain; the values in the literature range from 400 to 630 K.[24] This uncertainty affects the low-temperature values of $C_g(T)$ and consequently the derived values of $C_e(T)$. The value $\Theta(0) = 575$ K has been used in the following analysis both because it is considered the best value[25] and because it is the value determined by Feldman[23] in his analysis of the neutron-diffraction studies of the Cr phonon spectrum.

Blackman[26] has suggested that in general the form of $\Theta(T)$ appears to depend more on the elastic constants of the solid than on its actual crystal structure; he gives a plot of c_{12}/c_{11} vs c_{44}/c_{11} for a number of substances. If one takes Bolef and deKlerk's values of these constants,[27] the result indicates that Θ(Cr) should resemble that of NaCl.

TABLE I. Grüneisen constant.

T (K)	V (cm^3/mole)	β (K^{-1}) (10^{-5})	κ (cm^2/dyn) (10^{-13})	C_p (J/mole K) (10^1)	A (mole/J)
200	7.23	1.64	7.24	2.01	6.64×10^{-7}
400	7.23	2.46	5.46	2.61	1.18×10^{-6}

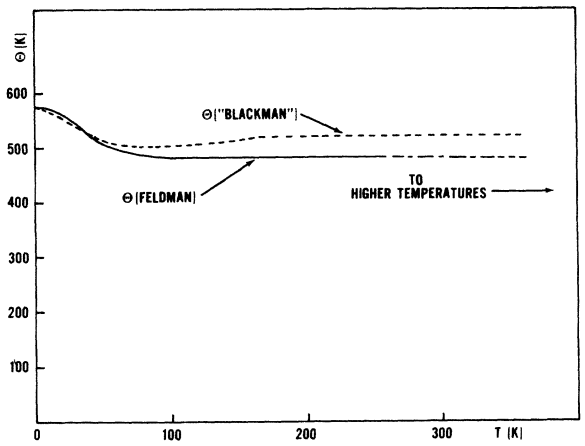

FIG. 2. Temperature dependence of the Debye temperature Θ of Cr. Θ(Feldman) is the dependence found by Feldman from analysis of the Cr phonon spectrum. Θ(Blackman) is the dependence found by using a suggestion of Blackman which results that $\Theta(T)$ would be similar to Θ(NaCl) in form.

$\Theta(T)$ for NaCl normalized to $\Theta(0) = 575$ K is shown in Fig. 2 compared with Feldman's result. While the two curves are similar at low temperatures, Feldman's $\Theta(T)$ more resembles the form of that of Be and Mg than NaCl.

One favors Feldman's calculation, of course. However, the resulting calculated C_g is greater than the C_v given as data[15] in the neighborhood of 60 K. Therefore C_g is shown in Fig. 1 calculated by both the Feldman and Blackman $\Theta(T)$'s. In the following analysis the Feldman value of $\Theta(T)$ will be used to extract C_e from the data; but no attempt will be made to analyze the form of these data at low temperatures, and the model will not be forced through the values of C_e in the vicinity of the Néel temperature.

Since the calculations are relatively insensitive to the value of Θ at high temperatures, it has been assumed that it can be simply extrapolated to high temperatures as a constant. This assumption is not likely to be correct.[26]

Finally, it has been assumed that $\Theta(T)$ shows no striking anomaly near T_N because that seems to be a reasonable conclusion from the extensive alloy work of Heiniger.[19]

C. Electronic Component

The electronic heat capacity C_e, which was found by the substraction $C_v - C_g$, is shown in Fig. 1. At very low temperatures C_e has the form[28]

$$C_e = \gamma(0)T \ , \tag{2.5}$$

where

$$\gamma(0) = \tfrac{1}{3}\pi^2 K^2 N(\zeta) \ , \tag{2.6}$$

a product of a constant, the Boltzmann constant, and the density of states at the Fermi energy ζ, respectively. $N(E)$, here and throughout the paper, contains a factor of 2 for the electron spin. At higher temperatures C_e will have some other temperature dependence resulting from the actual form of $N(E)$ and finally will become constant when the electron gas becomes nondegenerate.[28] The temperature dependence for simple models of band structure have been carried out by Elcock and coworkers.[29]

In Cr the behavior of C_e is further complicated by the disappearance of a portion of the Fermi surface (the A surface) as a result of an antiferromagnetic interaction that causes a BCS-type gap to open over it at temperatures below T_N.[4,5] Heiniger, Bucher, and Muller[18,24] have shown by the measurement of the heat capacity of a series of Cr alloys at low temperatures that the remaining P surface is approximately half the total surface. Thus, in the antiferromagnetic state at very low temperatures $\gamma(0) = \gamma_P(0)$, the value for the P surface. The average of all the experimental values collected by Heiniger[24] is

$$\gamma_P(0) = 1.481 \text{ mJ/K}^2\text{mole} \ , \tag{2.7}$$

with a spread in value ranging from 1.39 to 1.62 mJ/K^{2}mole. By extrapolating their paramagnetic alloys to zero concentration of solute, they find from the same series of experiments that

$$\gamma_P(0) + \gamma_A(0) = 2.9 \text{ mJ/K}^2\text{mole} \ . \tag{2.8}$$

From these values one computes that the ratio of the density of states at the Fermi level of the two surfaces is at temperatures above T_N,

$$R = \gamma_A(0)/\gamma_P(0) = N_A(\zeta)/N_P(\zeta) = 0.96 \ , \tag{2.9}$$

with a spread in value about 0.8–1.1.

The simple value of C_e given by Eq. (2.5) is shown in Fig. 1 with the change in the $\gamma(0)$ value at T_N. The actual value of C_e differs from this simple value over almost the whole temperature range. This excess value of C_e is more clearly shown in Fig. 3 where it is plotted as

$$C_e/\gamma_P(0)T - 1 = \gamma(T)/\gamma_P(0) - 1 \ . \tag{2.10}$$

It is seen that this excess is increasing relative to $\gamma_P(0)$ even at temperatures above T_N. This observation was noted by Shimizu[14] and is independent of the choice of $\Theta(T)$ given in Sec. IIB, although the exact magnitude and temperature dependence is not. Finally, the relatively constant values shown in Fig. 3 between about 600 and 1000 K are not indicative of nondegeneracy because in that case $C_e/\gamma_P T$ would vary as $1/T$.

III. MATHEMATICAL FORMULATION

The electronic heat capacity of a simple metal consists of two contributions: the redistribution of carriers about the Fermi level and the shift of the Fermi level itself. A multiband metal has an additional contribution coming from the transfer of carriers between the bands.[30,31] While a complete mathematical formulation of this problem is rather complicated, the symmetry of the model to be analyzed enables it to be greatly simplified, for the latter two contributions vanish.

In order to take advantage of this symmetry it is necessary to reformulate the heat capacity in terms of the energy E about the Fermi energy:

$$E_b = E + \zeta \quad , \tag{3.1}$$

where E_b is the energy with respect to the lower band edge and ζ is the Fermi energy. The energy of the carrier system is

$$U_b = \int_0^\infty E_b N'(E_b) f'(E_b)\, dE_b \quad , \tag{3.2}$$

where $N'(E_b)$ is the density of states and $f'(E_b)$ is the Fermi-Dirac function. Since the number of carriers is

$$n = \int_0^\infty N'(E_b) f'(E_b)\, dE_b \quad , \tag{3.3}$$

the total energy of the system is just

$$U_b = U + n\zeta \quad , \tag{3.4}$$

where

$$U = \int_{-\zeta}^\infty EN(E) f(E)\, dE \quad . \tag{3.5}$$

Here $f(E) = (e^{E/KT} + 1)^{-1}$.

Since the model is symmetrical about the Fermi level, ζ itself is constant. For a single band where the carrier concentration n can also be presumed constant, the electronic heat capacity is just

$$C_e \equiv \left(\frac{\partial U_b}{\partial T}\right)_v = \left(\frac{\partial U}{\partial T}\right)_v = -\int_{-\zeta}^\infty \frac{E^2 N(E)}{T} \frac{\partial f}{\partial E}\, dE + \int_{-\zeta}^\infty E \frac{\partial N}{\partial T} f(E)\, dE. \tag{3.6}$$

A second advantage of this model symmetry is that there is no carrier transfer between bands; the carrier concentrations n_j of the bands are constant. Therefore, the total electronic heat capacity is just the sum of independent contributions of the form of Eq. (3.6).

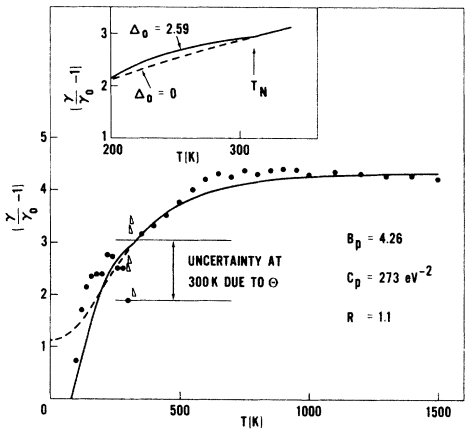

FIG. 3. Data for C_e plotted as $\gamma(T)/\gamma_0 - 1$ and the fit of the model to them. The data below $T_N = 312$ K have not been analyzed because of their uncertain worth, although the model does contain a term that could be used to fit them in principle. The parameters given are those of the model which yield the solid line. The dashed line is the prediction of the model for the case of paramagnetic Cr. The inset shows that there is an enhancement of Cr in the antiferromagnetic state just below T_N.

The lower limit of the integrals in Eq. (3.6) is the energy of the band edge beneath the Fermi energy. In order for the first integral to be independent of this band edge, the edge must be at least $15KT$ beneath the Fermi energy.[1,2] In other words to eliminate all band-edge effects, to preserve the symmetry of the model, and to obviate possibilities of nondegeneracy, the bandwidth must be at least $30KT$. At 1500 K this energy is about 3.6 eV. Gyorgy and Harvey[32] have determined a bandwidth of 7.2 eV by soft-x-ray techniques. Therefore, it is assumed in this problem that band edges are unimportant, although in a multiband problem this assumption is more stringent than a simple statement of bandwidth.

IV. MODEL

The model shown in Fig. 4 is similar to the one developed to explain the anomalies in the electrical and thermal conductivities of Cr that are seen between about 100 and 1000 K.[1-3] However, it is here presumed that the obvious energy dependence of that transport model arises from the density of states rather than group velocities or scattering. Accordingly the ordinant is taken as the reduced density of states $N(E)/N_P(0)$ rather than the reduced specific conductivity $\sigma(E)/\sigma_P(0)$. It should be realized that this assumption is only an approximation and that there are to be expected some differences in the values of the actual parameters of the model in the two cases. In the following analysis it will be attempted to retain the previous values of the

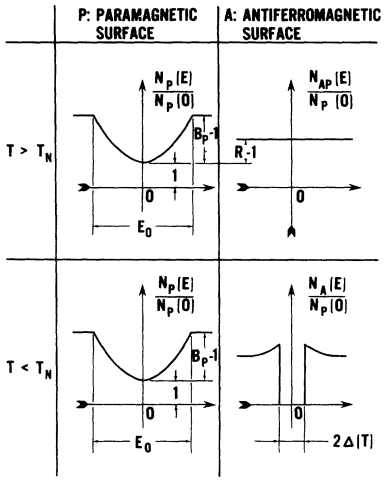

FIG. 4. Two-band model of the reduced density of states of Cr consisting of a paramagnetic P and an antiferromagnetic A surface. Below the Néel temperature T_N=312 K a BCS-type gap opens over the A surface.

parameters, which are given in Table II, as much as possible.

The model consists of two parts to account for the observation that the A portion of the surface disappears below T_N as a result of a BCS-type antiferromagnetic interaction. At all temperatures the remaining P surface is taken to be

$$N_P(E)/N_P(0) = 1 + C_P E^2 , \quad |E| < \tfrac{1}{2}E_0$$
$$N_P(E)/N_P(0) = B_P , \quad |E| \geq \tfrac{1}{2}E_0 . \qquad (4.1a)$$

This form was found necessary to explain the anomaly in the Lorenz number at temperatures above T_N. At $T \geq T_N$ the A surface is simply

$$N_A(E)/N_P(0) = R . \qquad (4.1b)$$

Since it will be found that the value of R differs in the transport and heat-capacity cases, it is of interest to define single-band values of the parameters in Eq. (4.1a):

$$B = (B_P + R)/(1 + R) ,$$
$$C = C_P(1 + R) . \qquad (4.2)$$

These relations allow the Lorenz number to be independent of R at these temperatures. In addition, the width of the well E_0 is independent of R:

$$E_0^2 = 4(B - 1)/C = 4(B_P - 1)/C_P . \qquad (4.3)$$

Below T_N the BCS gap opens over the A surface so that

$$N_A(E)/N_P(0) = R(E) = R|E|/[(E^2 - \Delta^2)^{1/2} + \delta], \quad |E| \geq \Delta \qquad (4.4)$$

$$N_A(E)/N_P(0) = 0 , \quad |E| < \Delta$$

where $\Delta = \Delta_0 KT_N(1 - T/T_N)^{1/2}$. The anisotropy factor δ [33] is set small and is used simply to eliminate the singularity in Eq. (4.4).

The model is completely symmetrical about the Fermi energy ($E = 0$) as long as band edges are unimportant. Therefore, as was pointed out in Sec. III, there is no charge transfer between these two surfaces. Thus,

$$C_e = C_{eP} + C_{eA} , \qquad (4.5)$$

where the C_{ej} are given by Eq. (3.6). At absolute zero $C_{eA} = 0$ for a nonzero value of Δ_0. C_{eP} then has the standard value

$$C_{eP} = \tfrac{1}{3}\pi^2 N(0) K^2 T \equiv \gamma_P(0) T . \qquad (4.6)$$

Thus, the γ ratio in Eq. (2.10) consists of three parts,

$$\frac{\gamma_P(T)}{\gamma_P(0)} = -\frac{3}{\pi^2}\int_{-\infty}^{+\infty} \epsilon^2 \frac{N_P(KT\epsilon)}{N_P(0)} \frac{\partial f}{\partial \epsilon} d\epsilon , \qquad (4.7a)$$

$$\frac{\gamma_A(T)}{\gamma_P(0)} = -\frac{3}{\pi^2}\int_{-\infty}^{+\infty} \epsilon^2 R(KT\epsilon) \frac{\partial f}{\partial \epsilon} d\epsilon , \qquad (4.7b)$$

$$\frac{\gamma_{AT}(T)}{\gamma_P(0)} = \frac{3T}{\pi^2 N_P(0)}\int_{-\epsilon_2}^{+\infty} \epsilon \frac{\partial N_A(KT\epsilon)}{\partial T} f\, d\epsilon , \qquad (4.7c)$$

where $\epsilon = E/KT$. The third term exists only below T_N.

At high temperatures the width of the well in the P surface in terms of reduced energy $\epsilon_0 = E_0/KT \to 0$. Therefore the limit of the γ ratio is

$$\lim_{T\to\infty} \frac{\gamma(T)}{\gamma_P(0)} = \lim_{T\to\infty}\left(\frac{\gamma_P(T)}{\gamma_P(0)} + \frac{\gamma_A(T)}{\gamma_P(0)}\right) = B_P + R , \qquad (4.8)$$

TABLE II. Parameters.

Quantity	Source: Conductivities Value	Conductivities Comment	Heat capacity Value	Heat capacity Comment
Δ_0	2.59	data fit	2.59	retained
E_0	0.218 eV	data fit	0.218 eV	retained
R	0.51	data fit	1.1	Heiniger (Refs. 18, 24)
B	2.55	data fit	2.55	retained
C	130 eV^{-2}	determined	130 eV^{-2}	retained
B_P	3.34	determined	4.26	determined
C_P	196 eV^{-2}	determined	273 eV^{-2}	determined

a constant, whereas a simple minimum in the density of states would vary as T^2. The data shown in Fig. 3 are approximately constant between 600 and 1500 K; the limiting value will be taken as 5.23.

The model parameters that were used to obtain the solid line fitting the data in Fig. 3 are given in Table II. The value of the zero-temperature BCS gap ratio was retained from the fit of the conductivities data because that value agrees with Barker's[6] value of $2\Delta_0 = 5.1$. Similarly, the value of E_0 was retained because that energy corresponds to an optical wavelength of about 6 μ, a value near the beginning of a temperature-independent structure in Barker's optical data. The single-band constants B and C have been retained because they together determine E_0 independent of R as can be seen by Eq. (4.3). The constants B_P and C_P are then determined by the choice of R and Eq. (4.2). Thus, only the constant R is adjusted to fit the data; its value $R = 1.1$ is in the range of values derived from Heiniger's data and given in Sec. IIC.

The fit to the data in Fig. 3 seems to be reasonable. The disagreement at temperatures near T_N is within the range of uncertainty resulting from the uncertainty in the value of Θ that was discussed in Sec. IIB. No attempt was made to use Eq. (4.7c) at temperatures below T_N for this same reason. However, it should be noted that there is indeed an excess of heat capacity above that accounted for by Eqs. (4.7a) and (4.7b) as one would expect.

The dashed line in Fig. 3 at temperatures below T_N is the prediction of the model for paramagnetic Cr; that is, Cr that has no gap on the A surface. One notes that just below T_N, C_e is enhanced in the antiferromagnetic state simply because there is a gap.

V. CONCLUSIONS

Klemens[34,35] has pointed out that one would expect to see the effect of band structure on the high-temperature transport properties of the transition metals for the simple reason that more and more of the band structure is enveloped by the Fermi skin as the temperature is raised. Goff[1-3] showed that in the case of Cr the anomalies seen in the conductivities above 100 K were ascribable to a quantity that had many characteristics of its band structure. By applying this model to an analysis of the electronic heat capacity, a quantity that depends solely on the density of states, this interpretation of the conductivity anomalies is substantiated.

Whereas the latter transition metals are known to agree with the Mott model[9] with its separate s and d bands, the earlier transition metals have long been thought to have hybridized sd or spd bands.[10,11,13] A consequence of the first-type band structure is that there would be no direct correlation between the conductivities and the electronic heat capacity because they would occur in different portions of it, the heat capacity going to the denser d bands. The hybridized band structure would be less likely to have extremely dense bands with the consequence that there would be an increased likelihood that the conductivities and the electronic heat capacity would be weighed toward the same electron group. The correlation between the models adduced to explain the anomalies in these two types of quantities indicates that there are no dense bands in Cr.

The model shown in Fig. 4 has been developed without resort to rigid-band considerations. It resembles Shimizu's[14] single rigid-band model to some extent but differs markedly by being symmetrical about the Fermi energy and by having no specified band edges. It was possible to escape specifying band edges because of the symmetry of the model. This neglect of band edges is consistent with the measured width of the band[32] but does not consider the effect of overlapping bands. Thus, while the A surface of the model is a standard band in the sense that it will give the usual value of the low-temperature coefficient of C_e, the P surface suggests two overlapping bands. It has been pointed out[2] that some features of the anomalies in the conductivities can be understood by using Gallo's formulation[36-38] for overlapping bands. In these terms one sees that the model implicitly considers the transfer of carriers between the two bands which comprise the P surface with no shift in the Fermi energy because of symmetry. Thus, the model is truly multiband. It is interesting to note that in the temperature range at which the carriers begin to be excited out of the well in the P surface the hardness of chromium[39] decreases rapidly.

There are at least two defects in the model shown in Fig. 4. The first, a minor observation, is that the shape of the P-surface well is probably too restrictive. The behavior of the data shown in Fig. 3 at temperatures between about 500 to 800 K implies that the well should vary faster than E^2. The second defect is more fundamental. Since theoretical treatment of the band structure of Cr and the antiferromagnetic transition[8] conclude that there is a shift of the Fermi energy during this transition, there should be some antisymmetry in the model. One sees from the agreement of the model with the data that this antisymmetry must be small.

ACKNOWLEDGMENTS

The author would like to thank Dr. J. R. Cullen and Dr. G. Heiche for their help in some mathematical parts of the problem.

[1]J. F. Goff, Natl. Bur. Std. (U.S.) Spec. Publ. No. 302, 311 (1968).
[2]J. F. Goff, Phys. Rev. B 1, 1351 (1970).
[3]J. F. Goff, Phys. Rev. B 2, 3606 (1970).
[4]T. M. Rice, A. S. Barker, Jr., B. I. Halperin, and D. B. McWhan, J. Appl. Phys. 40, 1337 (1969).
[5]D. B. McWhan and T. M. Rice, Phys. Rev. Letters 19, 846 (1967).
[6]A. S. Barker, Jr., B. I. Halperin, and T. M. Rice, Phys. Rev. Letters 20, 384 (1968).
[7]A. S. Barker, Jr. and J. A. Ditzenberger, Phys. Rev. B 1, 4378 (1970).
[8]S. Asano and J. Yamashita, J. Phys. Soc. Japan 23, 714 (1967).
[9]N. F. Mott, Proc. Phys. Soc. (London) 47, 571 (1935).
[10]W. Hume-Rothery and G. V. Raynor, *The Structure of Metals and Alloys* (Institute of Metals, London, 1962).
[11]W. Hume-Rothery, in *Electronic Structure and Alloy Chemistry of the Transition Elements*, edited by Paul A. Beck (Interscience, New York, 1963).
[12]L. D. Armstrong and H. Grayson-Smith, Can. J. Res. A28, 51 (1950).
[13]E. P. Wohlfarth, Rev. Mod. Phys. 25, 211 (1953).
[14]M. Shimizu, T. Takahashi, and A. Katsuki, J. Phys. Soc. Japan 17, 1740 (1962).
[15]*American Institute of Physics Handbook* (McGraw-Hill, New York, 1957), Sec. 4, pp. 40–42.
[16]R. H. Beaumont, H. Chihara, and J. A. Morrison, Phil. Mag. 5, 188 (1960).
[17]A. H. Sully, *Chromium* (Butterworth, London, 1954).
[18]F. Heiniger, E. Bucher, and J. Muller, Phys. Letters 19, 163 (1965).
[19]F. Heiniger, Phys. Kondensierten Materie 5, 285 (1966).
[20]M. W. Zemansky, *Heat and Thermodynamics* (McGraw-Hill, New York, 1943).
[21]M. E. Fine, E. S. Greiner, and W. X. Ellis, J. Metals 189, 56 (1951).
[22]A. H. Sully, Ref. 17, Table XVI, p. 85.
[23]J. L. Feldman, Phys. Rev. B 1, 448 (1970).
[24]F. Heiniger, E. Bucher, and J. Muller, Phys. Kondensierten Materie 5, 243 (1966).
[25]N. Wolcott (private communication).
[26]M. Blackman, in *Handbuch der Physik*, Vol. VII, edited by S. Flügge (Springer-Verlag, Berlin, 1955), Part I.
[27]D. I. Bolef and J. deKlerk, Phys. Rev. 129, 1063 (1963).
[28]A. H. Wilson, *The Theory of Metals* (Cambridge U. P., Cambridge, England, 1954).
[29]E. W. Elcock, P. Rhodes, and A. Teviotdale, Proc. Roy. Soc. (London) A221, 53 (1954).
[30]E. P. Wohlfarth, Proc. Phys. Soc. (London) 60, 360 (1948).
[31]E. P. Wohlfarth, Proc. Roy. Soc. (London) 195, 434 (1949).
[32]E. M. Gyorgy and G. G. Harvey, Phys. Rev. 87, 861 (1952).
[33]D. H. Douglass, Jr. and L. M. Falicov, in *Progress in Low Temperature Physics*, edited by C. J. Gorter (North-Holland, Amsterdam, 1964), Vol. IV.
[34]P. G. Klemens, Proceedings of the Fourth Thermal Conductivity Conference, San Francisco, 1964, paper Ia (unpublished).
[35]P. G. Klemens, in *Thermal Conductivity*, Vol. 1, edited by R. P. Tye (Academic, New York, 1969), p. 1.
[36]C. F. Gallo, R. C. Miller, P. H. Sutter, and R. W. Ure, Jr., J. Appl. Phys. 33, 3144 (1962).
[37]C. F. Gallo, B. S. Chandrasekhar, and P. H. Sutter, J. Appl. Phys. 34, 144 (1963).
[38]C. F. Gallo, J. Appl. Phys. 36, 3410 (1965).
[39]A. H. Sully, Ref. 17, Fig. 78, p. 154.

PHYSICAL REVIEW B VOLUME 4, NUMBER 4 15 AUGUST 1971

Interaction of Electrons with Impurities and the $k \approx 0$ Longitudinal Optical Phonon in Metal-Insulator-Semiconductor Tunnel Junctions*†

L. B. Schein‡ and W. Dale Compton§
University of Illinois, Coordinated Science Laboratory, Champaign-Urbana, Illinois 61801
(Received 1 February 1971)

Tunneling electrons have been observed to interact with phonons in metal-insulator-semiconductor (MIS) tunnel junctions including mass-defect phonons, $k \approx 0$ longitudinal and transverse optical phonons, and zone-boundary phonons. Well-known diffusion techniques have been used to introduce phosphorus into boron-doped silicon producing MIS tunnel junctions having two types of observable mass-defect phonons. These experiments suggest that the mass-defect phonons seen in tunneling arise from an interaction of tunneling electrons with screened, ionized impurity atoms in the reserve region of the semiconductor.

I. INTRODUCTION

Tunneling electrons have been observed to interact with phonons in metal-insulator-semiconductor (MIS) tunnel junctions. Interactions have been observed with local[1–3] and mass-defect[4] phonons, $k \approx 0$ longitudinal[1–3,5–8] and transverse[9] optical phonons, and zone-boundary phonons.[5] A central problem in the understanding of the MIS tunnel junctions is the identification of the mechanisms by which